Science of the Total Environment 951 (2024) 175351

Contents lists available at ScienceDirect

Science of the Total Environment

journal homepage: www.elsevier.com/locate/scitotenv

Use of isotopic (C, Cl) and molecular biology tools to assess biodegradation in a source area of chlorinated ethenes after biostimulation with Emulsified Vegetable Oil (EVO)

Sergio Gil-Villalba [a,*], Jordi Palau [a], Jesica M. Soder-Walz [b], Miguel A. Vallecillo [c], Jordi Corregidor [c], Andrea Tirado [c], Orfan Shouakar-Stash [d], Miriam Guivernau [e], Marc Viñas [e], Albert Soler [a], Monica Rosell [a]

[a] Grup MAiMA, SGR Mineralogia Aplicada, Geoquímica i Hidrogeologia (MAGH), Departament de Mineralogia, Petrologia i Geologia Aplicada, Facultat de Ciències de la Terra, Institut de Recerca de l'Aigua (IdRA), Universitat de Barcelona (UB), Martí Franquès s/n, 08028 Barcelona, Spain
[b] Departament d'Enginyeria Química, Biològica i Ambiental, Universitat Autònoma de Barcelona (UAB), Carrer de les Sitges s/n, Bellaterra, Spain
[c] Environmental Resources Management Iberia SAU, Rambla de Catalunya 33, 08007 Barcelona, Spain
[d] Isotope Tracer Technologies Inc., Waterloo, ON, Canada
[e] Sustainability in Biosystems Programme, Institute of Agrifood Research and Technology (IRTA), Torre Marimon, Caldes de Montbui, Barcelona, Spain

HIGHLIGHTS

- Carbon isotopic effects by partitioning of CEs into EVO were not significant.
- Biostimulation using EVO was studied in laboratory experiments and the field.
- *Dhc* populations and reductive dechlorination functional genes were analyzed.
- 2D C-Cl CSIA was used for degradation pathways investigation in the field.

GRAPHICAL ABSTRACT

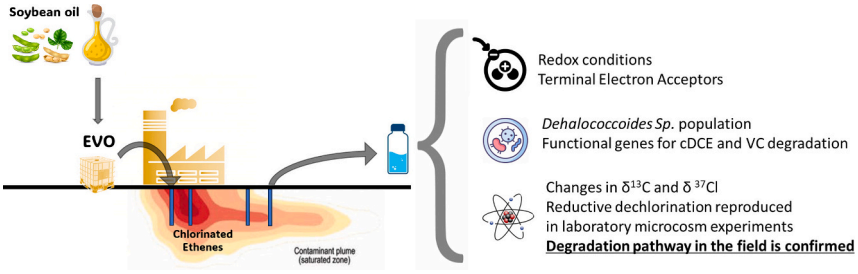

ARTICLE INFO

Editor: Elodie Passeport

Keywords:
2D-CSIA
Dichloroethene
EVO
Bioremediation
Microcosm study
Field application

ABSTRACT

Enhanced In Situ Bioremediation (EISB) using Emulsified Vegetable Oil (EVO) as a long-term electron donor has gained prominence for the treatment of groundwater contaminated with chlorinated ethenes (CEs). This study explores the potential of isotopic and molecular biology tools (MBT) to investigate the CEs (PCE, TCE and cis-DCE) bioremediation using EVO in a contaminated site. A multiple approach using C and Cl-CSIA, quantification of Dehalococcoides (Dhc) and specific reductive dechlorination (RD) gene population, and hydrochemical data in microcosm experiments and field samples was applied. Despite the high partitioning of CEs into the EVO phase, the carbon isotopic values of the remaining CEs fraction in the aqueous phase did not exhibit significant changes caused by phase partitioning in laboratory experiments. Both microcosm experiments and field data revealed a rapid RD of PCE and TCE, resulting in the transient accumulation of cis-DCE, which was slowly degraded to vinyl chloride (VC). These results agreed with the presence of Dhc populations and a shift to stronger reducing conditions in the field: i) RD functional genes (tceA, vcrA and bvcA) exhibited a trend to higher values and ii) a substantial increase in Dhc populations (up to 30% of the total bacterial populations) was observed over

* Corresponding author.
E-mail address: sergiogilv@ub.edu (S. Gil-Villalba).

https://doi.org/10.1016/j.scitotenv.2024.175351
Received 21 April 2024; Received in revised form 4 August 2024; Accepted 5 August 2024
Available online 14 August 2024

time. The dual-element isotope slope ΛC-Cl for RD of cis-DCE obtained from field data (ΛC – Cl = 5 ± 3) was similar to the one determined from the microcosm experiments under controlled anoxic conditions (ΛC – Cl = 4.9 ± 0.8). However, ΛC-Cl values differ from those reported so far for laboratory studies with Dhc strains and mixed cultures containing Dhc, i.e., between 8.3 and 17.8. This observation underscores the potential variety of reductive dehalogenases involved during cis-DCE RD and the importance of determining site-specific Λ and ε values in order to improve the identification and quantification of transformation processes in the field.

1. Introduction

Contamination of groundwater by chlorinated ethenes (CEs) has become a persistent environmental issue due to accidental releases and inappropriate historical disposal practices. In recent years, enhanced in situ bioremediation (EISB) techniques have emerged as reliable and cost-effective methods for treating these contaminants i) *Dhc* population relative to the total bacterial population and ii) functional genes related to RD (*tceA, bvcA* and *vcrA*). This suggests that the *Dhc* were most probably the drivers of RD in both the field and the microcosm experiments. Hence, the isotopic results obtained in the microcosm experiments might be representative for the analysis of biodegradation pathway and extent in the field.

However, the successful complete dechlorination of CEs through EISB is contingent upon achieving proper pH and oxidation-reduction potential (ORP) values, as well as the presence of organo-halide-respiring bacteria (OHRB) from the *Dehalococcoides* group (*Dhc*) and *Dehalogenimonas*. *Dhc* populations have been demonstrated as the key anaerobic and most common bacteria capable of transforming trichloroethylene (TCE), cis-dichloroethylene (cis-DCE) and vinyl chloride (VC) into non-toxic end products such as ethene and ethane under anaerobic conditions (Löffler et al., 2013; Chen et al., 2022b) via reductive dechlorination (RD). Failure to meet and sustain the mentioned conditions may result in an incomplete RD of CEs, causing the accumulation of degradation byproducts in the subsoil, i.e., cis-DCE and VC, which are more toxic than the original compounds. In this respect, VC ranks 4th on the 2022 Agency for Toxic Substances and Disease Registry Priority List of Hazardous Substances based on a combination of its frequency, toxicity, and potential for human exposure (ATSDR, 2023).

During RD of CEs, these are used as electron acceptors by OHRBs, while an electron donor is required to provide energy (Harkness and Fisher, 2013). Hydrogen (H_2) is commonly regarded as the primary electron donor for RD, which is typically generated through the anaerobic fermentation of carbon substrates by other native microbial populations. There is a wide range of commercially available electron donors, including soluble donors such as sugars, organic acids, and alcohols, as well as slow-release donors with low aqueous solubility like lactic acid polymers, emulsified vegetable oil (EVO), chitin, and wood chips (Leeson et al., 2004). These donors undergo microbial fermentation via different pathways and at different rates in groundwater under anaerobic conditions, leading to varying levels of hydrogen production and, thus, enhancing the growth and competitive advantage of OHRB against other hydrogen-consuming microorganisms (e.g. sulphate reducing bacteria and methanogens).

The RD of CEs by OHRB is catalyzed by diverse reductive dehalogenases (Rdh) which contain catalytic subunits (Ni et al., 1995; Magnuson et al., 2000). Rdh is a diverse protein family from which there are still a lot of unanswered questions regarding sequence diversity, substrate specificities, global distribution, and modes of inheritance (Hug, 2016). Nevertheless, the Rdh that have been characterized and proved to be functional in microbial respiration are encoded by Rdh operons, mainly composed by the *rdhA* and *rdhB* genes. The RdhA enzymes act as catalyst for cleaving the C-Cl bond during organohalide respiration (West et al., 2013; Badin et al., 2014). The expression of rdh genes has been established as a biomarker for the physiological activity of *Dhc* (Lee et al., 2008; Löffler et al., 2013; Blázquez-Pallí et al., 2019a). *PceA* gene is active for the RD of tetrachloroethylene (PCE) and both *tceA* and *vcrA* genes are active for that of TCE and cis-DCE. In addition, both *vcrA* and *bvcA* are primarily and exclusively responsible for the RD of VC to ethene under anaerobic conditions (He et al., 2005; Lee et al., 2008; Franke et al., 2020).

Compound-Specific Isotope Analysis (CSIA) is based on isotopic fractionation principles, where light isotopes (e.g., ^{12}C, ^{35}Cl) form and break bonds more readily than heavy isotopes (e.g., ^{13}C, ^{37}Cl) during (bio)chemical reactions. This results in a transient accumulation of heavy isotopes in the remaining pool of the parental organic compound due to slower reaction kinetics. CSIA leverages these variations to trace sources and transformation pathways of halogenated compounds in groundwater (Nijenhuis et al., 2016). This approach has gained significant interest in site investigation and remediation practices as it provides complementary lines of evidence for contaminant biodegradation, which are sometimes required by legislation and regulatory administrations (Nijenhuis et al., 2007; Aelion et al., 2009; Elsner, 2010; Palau et al., 2014). In contrast to the single element isotope approach, the application of dual-element isotope analysis (2D-CSIA) has demonstrated high potential for identifying the contaminant degradation pathways in the field (Wiegert et al., 2012; Blázquez-Pallí et al., 2019b; Rosell et al., 2019). By measuring the isotopic shifts of different elements in the same compound (e.g., C and Cl), specific ongoing degradation mechanisms can be identified (Elsner, 2010; Hermon et al., 2018). However, before the degradation mechanisms can be confidently identified in the field, it is crucial to characterize their specific isotopic fractionation values (εC and εCl) and dual-element isotope trends ($\Lambda^{C\text{-}Cl}$) in laboratory experiments under controlled conditions (Aelion et al., 2009).

Emulsified Vegetable Oil (EVO) is a commercially available bioremediation substrate which consists of an emulsion of soybean oil, surfactants, soluble substrates (e.g., lactate), and nutrients (Newman and Pelle, 2006; Harkness and Fisher, 2013). Due to its low aqueous solubility and composition, that includes soybean oil containing long-chain fatty acid groups, EVO undergoes slow fermentation over time, producing hydrogen and volatile fatty acids. In contrast to more soluble donors, the slow fermentation of EVO prevents the need for its continuous or semi-continuous injection (Lalman and Bagley, 2000; Harkness, 2000). The injection of vegetable oil in the subsurface of a contaminated site can lead to abiotic processes such as the partitioning of CEs into oily phases. These phenomena can cause significant changes of the concentration of CEs in groundwater (Yang and Mccarty, 2000; Pfeiffer et al., 2005), hampering the evaluation of biodegradation by using contaminant concentration data alone.

The isotopic effect of physical processes on organic compounds (e.g. sorption and diffusion) has often been disregarded in the saturated zone, due to their expected small effects compared to biodegradation (Abe et al., 2009; Audí-Miró et al., 2013; Torrentó et al., 2017; Rodríguez-Fernández et al., 2018). Specific studies on sorption and diffusion demonstrated that they could compensate each other to some degree as these processes fractionate isotopes in opposite directions. However, when strong sorption dominates in the field, carbon isotope fractionation of volatile chlorinated compounds can become significant ≥2 ‰, which might need to be considered for an accurate interpretation of reactive processes using CSIA (Höhener and Yu, 2012; Wanner et al., 2017; Halloran et al., 2021). To the best of our knowledge, there is only one study documenting the water-vegetable oil phase partitioning of CEs (Pfeiffer et al., 2005) and the potential isotopic fractionation caused by

this process has not been evaluated so far. Therefore, the investigation of potential isotope effects during partitioning of CEs into EVO is warranted.

Previous studies have investigated the application of EVO as an electron donor for CEs bioremediation in laboratory experiments (Long and Borden, 2006; Lee et al., 2007; Harkness and Fisher, 2013; Hiortdahl and Borden, 2014; Yu et al., 2018; Underwood et al., 2022). However, research dealing with contaminant remediation using EVO in the field is still limited (Hirschorn et al., 2007; Révész et al., 2014; Chen et al., 2022a). These previous studies provide insights into certain effects of RD after the injection of an electron donor, namely acidification of groundwater and changes in microbial community dynamics. As far as we know, only two studies have used the carbon isotopic fractionation of CEs to assess the efficiency of the biostimulation with EVO (Hirschorn et al., 2007; Révész et al., 2014). Currently, there is still a knowledge gap regarding the potential of 2D-CSIA to investigate the fate of PCE, TCE, and cis-DCE following an EVO injection in the field. In particular, the dual (C, Cl) isotope analysis could be useful to identify the degradation pathway of cis-DCE, which can be transformed via both microbial anaerobic RD and aerobic oxidation (Tiehm and Schmidt, 2011). Besides, contrarily to PCE and TCE, few studies have reported the dual-element (C, Cl) isotope fractionation trend for cis-DCE during RD (Abe et al., 2009; Kuder and Philp, 2013; Doğan-Subaşı et al., 2017; Lihl et al., 2019).

The main goal of this study was to explore the potential of a multi-method approach (i.e. isotopic and biomolecular tools) to improve the assessment of CEs degradation by EISB with EVO. To this end, we investigated (i) whether water – EVO phase partitioning processes of CEs result in significant isotopic effects; (ii) the C and Cl isotopic fractionation and dual (C, Cl) isotope trends of PCE, TCE and cis-DCE during RD in microcosm experiments with a bacterial community from the contaminated site; (iii) the dual (C, Cl) isotope fractionation trend of cis-DCE during the EISB with EVO in the field; and (iv) the *Dhc* bacterial populations and functional genes responsible for RD of CEs in both microcosm experiments and field samples. Finally, the isotopic fractionation values and dual element isotope trends were compared with the available literature data.

2. Material and methods

2.1. Study site

The study site, located near Barcelona (Spain), was strongly contaminated with PCE (reaching a value of 19 mg/L in groundwater), due to former improper storage and handling practices. The unconfined aquifer layer consists of a Quaternary sand and sandy-silt bed with a thickness ranging between 4 and 8 m. Below this unit, Miocene detrital deposits of alternating clay and silt layers represent the bottom of the aquifer (bedrock). The groundwater flows toward the southeast, following the dip of the Quaternary/Miocene contact. The water table depth ranges between 2 and 4 m below ground surface. Hydraulic conductivity values between 0.25 and 0.35 cm/s and transmissivity ranging from 0.8 to 1.7 m^2/day were determined through pumping tests.

2.2. EVO injection details

A commercial EVO (EOS PRO®, EOS Remediation, LLC, Research Triangle Park, North Carolina, USA) was selected as a long-term electron donor for the site bioremediation. It is a physical emulsion consisting of soybean oil in water, vitamin B_{12} and other minor substances as emulsifiers and nutrients.

The EVO injection was conducted in eight wells (Fig. 1). The injection process involved the sequential injection of 13 m^3 of an EVO solution (8 % *v*/v), followed by 5.6 m^3 of an aqueous lactate solution (5 % v/v). Lactate is a more soluble and mobile electron donor, and this solution was used to induce anoxic conditions in a shorter term. Both solutions were prepared using tap water, previously circulated through an activated carbon filter to remove any potential volatile halogenated compound that can result from the chlorination process and free chlorine (Cl_2) which could kill a wide range of bacteria.

2.3. Collection of water samples

The site was equipped with 20 long screen wells installed in 2010. Eleven monitoring wells, located on the source and downgradient areas (Fig. 1) were selected for the assessment of the potential natural attenuation of CEs before the EVO injection and the evolution of the contamination after the biostimulation treatment. To do so, an initial groundwater sampling campaign was carried out in June 2020, followed by the injection of EVO (September 2020) and five monitoring campaigns (November 2020, January, March, May, and September 2021). Slurry was sampled for biomolecular analysis in four injection wells (W4, W8, W10 and W11) and one control well (W5) in June 2020 (3 months before the EVO injection), in March 2021 (6 months after the injection) and only in W4 in June 2021 (Table 1). Hydrochemical parameters, including temperature, pH, electric conductivity, Dissolved Oxygen (DO), and ORP, were measured on-site, before each sampling, using a multiparameter probe (HANNA HI98194 and sensors HANNA HI7698194) together with a flow-through cell to minimize contact of the sample with the atmosphere. Data were collected after stabilization and ORP values were corrected to the standard hydrogen electrode (SHE). For CEs concentration and isotopic analyses, triplicate groundwater samples were collected in amber glass bottles (125 mL) filled without headspace (HS) and closed with screw PTFE-lined septum caps to minimize adsorption and volatilization of CEs. The samples were preserved by adding concentrated HNO_3 (to pH < 2) and stored in the dark

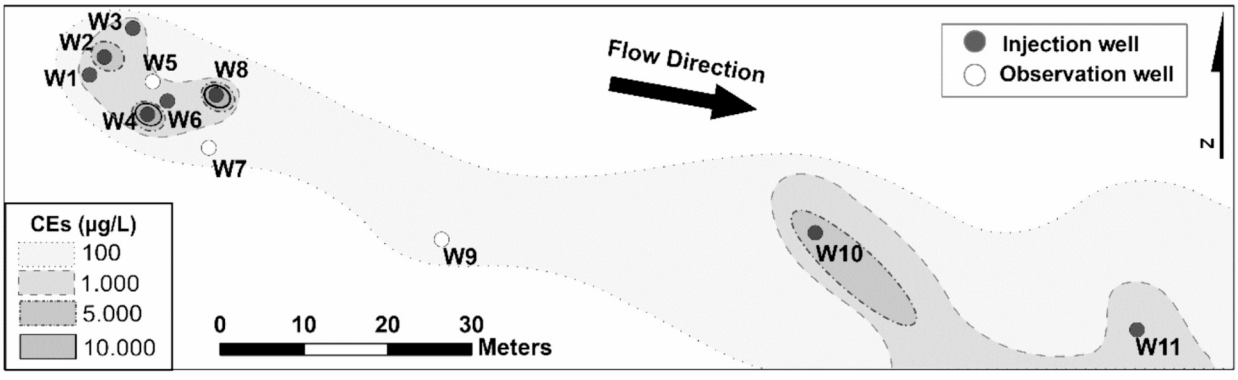

Fig. 1. Site map and groundwater monitoring wells network. The filled contour lines represent the total CEs concentrations in groundwater (in µg/L) prior to the injection (June 2020).

Table 1
qPCR results for groundwater samples and microcosm regarding total bacterial population (16S rRNA), *Dehalococcoides* ssp. and functional genes *tceA, bvcA* and *vcrA*. All analyses were performed in triplicate. n.a. and n.d. stand for not analyzed and not detected, respectively. Different subscript letters in each gene population represents significant differences ($n = 3$, $P < 0.05$, Post Hoc Tukey tests).

Field data							
Well	Date	Gene copies 16S rRNA mL^{-1}	Gene copies 16S rRNA *Dhc* mL^{-1}	% *Dhc*	Gene copies *tceA* mL^{-1}	Gene copies *bvcA* mL^{-1}	Gene copies *vcrA* mL^{-1}
W4	Jun-20	$1.14E+05_a$	$1.10E+03_a$	1.0	$8.57E+01_a$	$9.13E+01_a$	$3.77E+03_a$
W4	Mar-21	$1.04E+05_a$	$1.40E+04_b$	13.5	$3.83E+04_b$	$2.00E+04_b$	$3.75E+04_b$
W4	Jun-21	$1.67E+06_b$	$1.97E+05_c$	11.8	$1.08E+06_c$	$3.02E+05_c$	$1.19E+06_c$
W5	Jun-20	$4.76E+04_a$	$2.88E+00_d$	0.0	n.a.	n.a.	n.a.
W5	Mar-21	$2.05E+06_b$	$2.89E+04_b$	1.4	n.a.	n.a.	n.a.
W8	Jun-20	$1.49E+04_c$	$4.17E+00_d$	0.0	n.a.	n.a.	n.a.
W8	Mar-21	$1.36E+07_d$	$4.19E+06_e$	30.8	$1.78E+07_d$	$1.55E+06_c$	$3.53E+06_c$
W10	Jun-20	$1.12E+05_a$	$4.77E+01_d$	0.0	n.d.	n.d.	n.d.
W10	Mar-21	$1.79E+07_d$	$1.02E+06_e$	5.7	$5.18E+06_e$	$1.09E+02_d$	$3.83E+06_c$
W11	Jun-20	$7.59E+02_e$	$1.50E+01_d$	2.0	n.a.	n.a.	n.a.
W11	Mar-21	$1.46E+07_d$	$8.95E+04_{bc}$	0.6	n.a.	n.a.	n.a.
Microcosm experiments							
Microcosm	**Degradation (%)**	**Gene copies 16S rRNA mL^{-1}**	**Gene copies 16S rRNA *Dhc* mL^{-1}**	**% *Dhc***	**Gene copies *tceA* mL^{-1}**	**Gene copies *bvcA* mL^{-1}**	**Gene copies *vcrA* mL^{-1}**
cDCE (t_0)	0	$1.67E+06_b$	$1.97E+05_c$	11.8	$1.08E+06_c$	$3.02E+05_c$	$1.19E+06_c$
cDCE_1 (t_1)	58	$9.70E+05_b$	$7.02E+03_{ab}$	0.7	$7.61E+04_b$	$1.12E+04_b$	$2.92E+04_b$
cDCE_2 (t_2)	98	$4.81E+06_{ab}$	$7.03E+06_e$	>70	$8.66E+06_c$	$4.12E+05_c$	$6.11E+06_c$

at 4 °C until analysis. Slurry for the microcosm experiments was collected from the bottom of the well W4 in June 2021. This well was selected for microcosm preparation because it presented the highest CEs concentrations and bacterial populations in the sampling before the injection (June 2020).

2.4. Partitioning experiments

Experiments were conducted to assess whether the potential partitioning of CEs between the water and EVO phases result in significant isotopic fractionation. The experimental setup (total volume of 140 mL) consisted of two polypropylene syringes connected through a 14,000 Da dialysis membrane (Medicell Membranes Ltd., London, UK), permeable to CEs while impermeable to EVO (see Fig. S1, in SI). One side of the system was filled with an aqueous EVO solution (8 % *v*/v) and the other with an aqueous solution (PCE, TCE and cis-DCE) leading to initial concentrations in the system of 1570 μg PCE/L, 2290 μg TCE/L and 2750 μg cis-DCE/L. All solutions were prepared using deionized water (18.2 MΩ cm at 25 °C, Direct-Q UV-3, Millipore) and their concentrations were selected to be in the range of those present in the field during the EVO injection. Both sides of the system were stirred during the experiment using PTFE-coated magnetic stir bars to ensure the homogeneity of the solutions. The syringe tips were capped and all connections were sealed with PTFE tape and Parafilm® to minimize losses of CEs by volatilization. Two water samples (5 mL) were collected after 12 and 48 h from the side of the system filled with the CEs solution (without EVO). The water samples were stored, without headspace, in amber vials with PTFE-sealed caps, and refrigerated until concentration and isotopic analysis. The dialysis membrane prevented the presence of EVO phase in the samples as it could provoke the release of CEs from the EVO to the water during the heating of the samples in subsequent analyses. Experiments were performed in triplicates to ensure reproducibility. Control triplicates without EVO were included to account for possible losses in the system. The calculation of the partition to EVO is detailed in Appendix B of SI.

2.5. Microcosm experiments

Laboratory microcosm experiments were conducted in order to obtain field site-specific $\varepsilon^{13}C$, $\varepsilon^{37}Cl$, and $\Lambda^{C\text{-}Cl}$ values for the RD of PCE, TCE and cis-DCE. Initially, the collected slurry from the well W4 on June 2021 (9 months after EVO injection) was purged with N_2 for 3 h to remove CEs. Subsequently, the microcosms were prepared inside an anoxic chamber filling 100 mL glass serum sterile bottles with 70 mL of slurry and sealed with PTFE-coated butyl rubber stoppers and aluminum crimp caps. Three sets of 13 bottles each were spiked with PCE, TCE, or cis-DCE respectively at 160 μM. Ten bottles of each set were amended with lactate (3 mM) to assess the effect of a supplementary electron donor while 3 bottles remained in field conditions. Three additional killed control bottles were spiked with all the contaminants together (PCE, TCE, and cis-DCE) and the biodegradation activity was immediately stopped by adding a solution of NaOH (to pH > 12). The killed controls were set up to account for contaminant losses through the cap or unexpected abiotic reactions. All these bottles were incubated in the dark at 25 °C. The concentration was monitored on a daily basis by injecting 0.5 mL of microcosm HS in a Gas Chromatograph coupled to a Flame Ionization Detector (GC-FID). Biodegradation was stopped at different degradation extents to assess the associated isotopic fractionation by adding NaOH, as described previously.

In those cases where the rapid kinetics led to the complete biodegradation of the original compound before sufficient data could be obtained for the calculation of ε-values, the corresponding CE was spiked again, and subsequent sampling was performed. When multiple spikes were conducted and degradation products (particularly cis-DCE) accumulated, microcosm bottles were purged with N_2 for 20 min prior to the following spike. This precautionary step was taken based on previous studies that observed inhibition of RD at high CEs concentrations (Duhamel et al., 2002).

2.6. Analytical methods

2.6.1. Concentration

A detailed description of the analytical methods and equipment used for concentration and isotope measurements is available in the SI. Briefly, CEs concentrations in field samples were measured by headspace gas chromatography–mass spectrometry (HS-GC–MS) as explained elsewhere (Torrentó et al., 2017) while CEs and ethene concentrations in microcosm samples were measured by a GC attached with a FID at UAB laboratories. Terminal Electron Acceptors (TEAs) concentrations such as nitrate, sulphate, manganese, and iron in field samples were analyzed by Element Materials Technology (EMT), Deeside, United Kingdom (see SI).

2.6.2. Isotopic analysis

Carbon isotope analysis of PCE, TCE cis-DCE and VC was performed using a GC coupled to an Isotope Ratio Mass Spectrometer (GC-IRMS) at

the Technological Centers of the University of Barcelona (CCiT-UB) (Blázquez-Pallí et al., 2019a). Aqueous isotopic working standards of CEs with known isotopic composition were analyzed on a daily basis to ensure stability of the measurements during the course of samples analysis and, if necessary, to correct for slight deviations induced by the extraction and preconcentration technique (solid-phase micro extraction -SPME (Palau et al., 2007)). Chlorine isotope analysis of PCE and TCE was performed in a GC-qMS system in the CCiT-UB using the methodology described by (Jin et al., 2011), while chlorine isotope ratios of cis-DCE were analyzed using a GC-IRMS at Isotope Tracer Technologies Inc. (Waterloo, Canada) as described in (Shouakar-Stash et al., 2006). Raw $\delta^{37}Cl$ values were calibrated (two-point linear calibration) to the standard mean ocean chloride (SMOC) scale (Bernstein et al., 2011). For both C and Cl isotope analysis, samples and standards were analyzed by a duplicate set of injections as quality control (2 injections in the GC-IRMS and 2 sets of 5 injections in the GC-qMS). The aqueous isotopic standards were prepared similarly to the samples and measured in the same sequence. Precision (1σ) of the analysis was ≤0.5 ‰ for $\delta^{13}C$ of all compounds and for $\delta^{37}Cl$ of PCE and TCE, and ≤0.2 ‰ for $\delta^{37}Cl$ of cis-DCE.

Recent studies by (Ojeda et al., 2019, 2020) suggested to use the York regression method instead of ORL to determine Λ and its uncertainty. A comparison between $\Lambda^{C\text{-}Cl}$ values and their uncertainties obtained in this study with the York and the OLR regression methods will be conducted.

2.6.3. Biomolecular analysis

Biomass was harvested, either from 30 mL of field-sampled slurry or 5 mL samples from selected microcosm experiments, in sterile falcon tubes that were centrifuged at 4000 ×*g* and 4 °C for 30 min. The supernatants were discarded, and the resulting pellets were immediately stored at −80 °C until DNA extraction. DNA extraction was performed using the DNeasy PowerSoil Pro Kit (Qiagen, Venlo, The Netherlands), following the manufacturer's instructions.

The RD genes quantified were: i) *tceA* gene, encoding for the RD enzyme of TCE to cis-DCE; ii) *vcrA* gene, encoding for VC reductase enzyme responsible for RD of cis-DCE and VC; and iii) *bvcA* gene, encoding for VC reductase enzyme responsible for RD of VC to ethene, as described elsewhere (van der Zaan et al., 2010).

2.7. Isotope data evaluation

The carbon and chlorine isotopes ratio were reported in delta notation ($\delta^{h}E$, in ‰, Eq. (1)), relative to the international standards VPDB (Vienna Pee Dee Belemnite) and SMOC (Standard Mean Ocean Chlorine) (Kaufmann et al., 1984; Coplen, 1996), respectively. The isotopic ratio of a sample and the standard of an element (E) (e.g., $^{13}C/^{12}C$, $^{37}Cl/^{35}Cl$) is denoted as R_{sample} and R_{std}, respectively:

$$\delta^{h}E = \left(\frac{R_{sample}}{R_{std}} - 1\right) \quad (1)$$

A simplified version of the Rayleigh equation in logarithmic form (Eq. (2)) can be used to correlate changes in the isotopic composition of an element in a compound (R_t/R_0) with changes in its concentration ($f = C_t/C_0$) for a given reaction, by using the corresponding isotopic fractionation (ε) (Elsner, 2010; Coplen, 2011):

$$ln\left(\frac{R_t}{R_0}\right) = \varepsilon \cdot ln(f) \quad (2)$$

where R_t/R_0 can be expressed as $(\delta^{h}E_t + 1)/(\delta^{h}E_0 + 1)$ according to the $\delta^{h}E$ definition. The laboratory-derived ε values according to Eq. (2) were compared to reported values in the literature. The dual isotope analysis was used to investigate the reaction pathways of CEs by comparing the slopes obtained in the laboratory with those observed in the field. The $\Lambda^{C/Cl}$ values for PCE, TCE and cis-DCE in the field and laboratory experiments were obtained from the slope of the linear regression in the dual C-Cl isotope plot (Elsner, 2010). The results were also compared with $\Lambda^{C/Cl}$ values from the literature. The uncertainty of ε and $\Lambda^{C/Cl}$ values is reported as the 95 % confidence interval (CI), derived from the standard deviation of the regression slope.

3. Results and discussion

3.1. Carbon isotopic effect during water - EVO phase partitioning

The extent of CEs partitioning into the EVO phase in the laboratory tests was estimated based on the difference in the measured aqueous concentrations between the experiments with EVO and the controls without it (see details in SI). After 48 h the experiments with EVO showed a decrease in aqueous concentrations around 83 %, 69 % and 65 % for PCE, TCE and cis-DCE, respectively, compared to the controls. These results reflected a significant partitioning of CEs into the EVO phase and were consistent with the trend to higher transfer with increasing chlorination of CEs determined in a previous study using food-grade soybean oil and synthetic groundwater (Pfeiffer et al., 2005). These authors determined soybean oil - groundwater partition coefficients (L water/L oil) of 539, 351 and 56 for PCE, TCE and cis-DCE, respectively, in a CEs solution with PCE, TCE, cis-DCE and vinyl chloride at 20 °C.

Despite the high partitioning of CEs into the EVO phase, the carbon isotopic values of the remaining CEs fraction in the aqueous phase did not exhibit significant differences between control and EVO experiments. Although low concentrations did not allow the measurement of $\delta^{13}C$ of PCE, nor for all the triplicates of TCE and cis-DCE, a change in the isotopic composition was not observed for TCE or cis-DCE after 48 h (Fig. 2). These results suggest that the carbon isotopic effect of the partitioning of these compounds into EVO during field applications will be small or insignificant compared to the biodegradation of the CEs in the groundwater.

3.2. CEs biodegradation in the microcosm experiments

Complete biodegradation of PCE, TCE and cis-DCE was observed in all active microcosm experiments (see Figs. S3, S4 and S5, in SI), while the concentrations in the killed controls remained unchanged. In microcosm bottles without lactate addition, no significant differences in biodegradation dynamics were observed (treated equally hereinafter and in the graphs). This can be attributed to the fact that the used slurry was already biostimulated, sampled after 9 months of EVO injection. This observation demonstrates that EVO serves as a long-term carbon source, indicating that the availability of an electron donor is not a limiting factor for RD in the microcosm experiments where lactate was not added.

Following a latency period of about 48 h after PCE and TCE were spiked (Figs. S3 and S4, in SI), rapid biodegradation was observed, as these compounds were completely depleted after 96 h. In this case, re-spiking of the compounds was necessary to obtain samples at different degradation extents for the calculation of ε-values. When it was necessary, the microcosms were purged to prevent inhibition of OHRB due to toxicity caused by the accumulation of degradation products as this process has been previously documented by (Duhamel et al., 2002). Unlike PCE and TCE, cis-DCE microcosms did not exhibit a latency period and its degradation rate was slower, requiring around 16 days to complete the transformation of cis-DCE into VC (Fig. 3). This longer biodegradation period allowed for detailed sampling, representative of different extents of cis-DCE transformation (Fig. S5, in SI). The absence of a lag phase for cis-DCE might be attributed to the fact that cis-DCE and VC were already the predominant contaminants in the sampled slurry, rendering the functional genes for PCE and TCE degradation inactive.

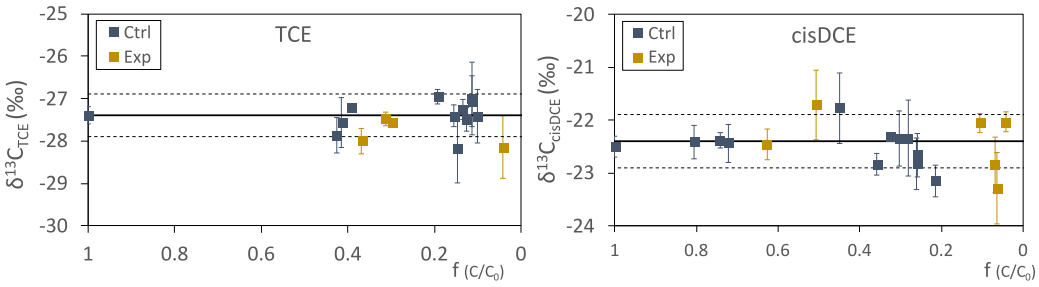

Fig. 2. Carbon isotopic values of CEs in the aqueous phase versus time in the EVO-phase partitioning experiments (yellow) and controls without EVO (dark blue). The black line indicates the carbon isotopic composition of the original compound (measured by Elemental Analyzer - IRMS) and the dashed lines show the typical analytical uncertainty of ±0.5 ‰.

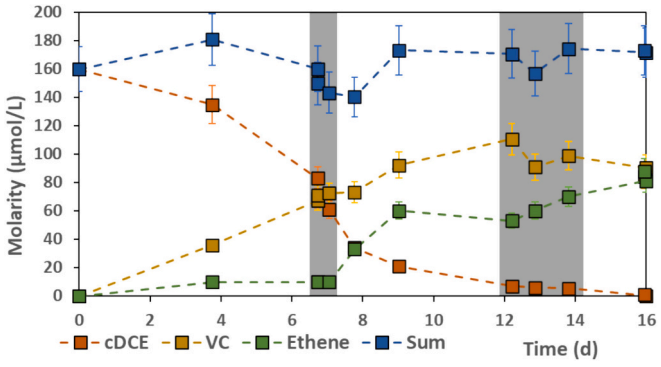

Fig. 3. Molarity of original compound and degradation products in microcosms amended with cis-DCE (160 µM). The shaded areas indicate the microcosms sampled for subsequent microbiological analysis.

3.3. Geochemical conditions and CEs biodegradation in the field

In general, groundwater was characterized by anoxic conditions prior to the injection, with DO values close to 0 mg/L in all measurements, except for well W6 with 0.29 mg/L. Other redox-sensitive species, such as nitrate and sulphate, with concentrations up to 33 mg/L and 125 mg/L, respectively, before the injection (June 2020) were strongly depleted by March 2021 (Fig. S6, in SI). On the other hand, dissolved manganese and methane concentrations strongly increased (even in observation wells such as W9 located downstream from the source area), with some wells showing methane concentrations exceeding 20 mg/L (Fig. S6, in SI). This shift to stronger reducing conditions after the EVO injection, which fall within the range of sulphate-reducing to methanogenic conditions, was favourable for RD of CEs (Leeson et al., 2004). Also, pH and ORP values presented optimal conditions for RD (see further discussion in SI).

Regarding the concentration of CEs, prior to the EVO injection (June 2020) PCE and TCE were the predominant CEs in the contaminated area, accounting for 50 to 90 % of the dissolved CEs molar concentration (Fig. 4). However, the presence of the dechlorination products cis-DCE and VC (in some wells) was indicative of PCE and TCE natural attenuation to some extent, in agreement with the anoxic conditions observed previous to the EVO injection (Fig. S6, in SI). Two months after the injection, the degradation products cis-DCE and VC were already predominant in all the wells, accounting for nearly 100 % of the dissolved CEs. The average measured PCE and TCE concentration dropped from 4599 to 44 µg/L and from 3074 to 37 µg/L, respectively. Conversely, the degradation products average concentrations increased from 3323 to 22,082 µg/L for cis-DCE and from 1515 to 4035 µg/L for VC.

The analysis of the total molarity of CEs showed, in most of the wells, an increase after the injection (Fig. 4). This phenomenon has been previously observed in other EVO field applications (Révész et al., 2014) and it could be caused by the mobilization of remaining DNAPL or adsorbed CEs on the aquifer material. In the studied site, this mobilised DNAPL could have been rapidly degraded to cis-DCE once dissolved in the aqueous phase, as rapid biodegradation rates were observed in microcosm experiments, causing the high cis-DCE concentrations measured after the injection. On the other hand, wells W4 and W8 showed significantly higher concentrations than the other wells, which might indicate that DNAPL existed nearby. Additionally, well W11 was the only one which presented high PCE and TCE molar fractions in the following campaigns, until March, while on W9 PCE and TCE where not found in the November monitoring, but a rebound was observed in March and May. Finally, the total CEs concentration decreased significantly in all wells in September 2021, apart from the well W1, where an increase in the total molarity of CEs was observed.

The rapid transition to a system dominated by degradation products cis-DCE and VC indicate that PCE and TCE are rapidly transformed at the site, in agreement with the fast PCE and TCE biodegradation observed in the microcosm experiments (see above). However, other processes such as partitioning of CEs to the injected EVO phase (higher for PCE and TCE compared to cis-DCE, see Fig. 3) and CEs mobilization/desorption during the EVO injection can also affect the parent compounds/daughter products ratios. Therefore, the use of isotopic and biomolecular tools to document CEs transformation in complex systems, like the in-situ biodegradation using EVO, is warranted. In most wells, a slow decrease of cis-DCE molar fraction is observed over time, transitioning to a VC-dominated system. In this scenario, the assessment of cis-DCE (and VC) transformation is crucial to evaluate the effectiveness of the biostimulation treatment. Overall, concentration data indicate that the injection of EVO enhances the degradation of PCE and TCE within a relatively short timeframe, while the degradation kinetics of cis-DCE to VC is slower.

3.4. Microbiological analyses in microcosms and the field samples

For the microcosm experiments, only the data from those spiked with cis-DCE are discussed. For the experiments with PCE or TCE correlating microbiological activity with the degradation of the respective parent compound was not possible due to their rapid biodegradation, as well as the re-spikes and purges (see above). Additionally, the limited number of samples hindered the analysis of triplicates with similar extent of degradation. In contrast, the slower degradation of cis-DCE allowed for more extensive sampling and triplicate qPCRs were conducted for 60 % degradation after 7 days (t_1), and over 97 % degradation after 12 days (t_2). Original triplicates of unpurged groundwater collected from W4 well (Fig. 1) were also analyzed as the initial value (t_0).

At t_1, the population of *Dhc* and Rdhase abundance slightly decreased (10 %, $P > 0.05$) compared to the initial value (Table 1). This *Dhc* decline, along with a significant total bacterial population drop, could have been caused by purging disturbance and a period of absence of CEs until they were spiked. Similar observations of decay in *Dhc* populations and Rdhs gene population due to the absence of CEs have been previously reported by (Lee et al., 2006). Contrastingly, at t_2 the *Dhc*

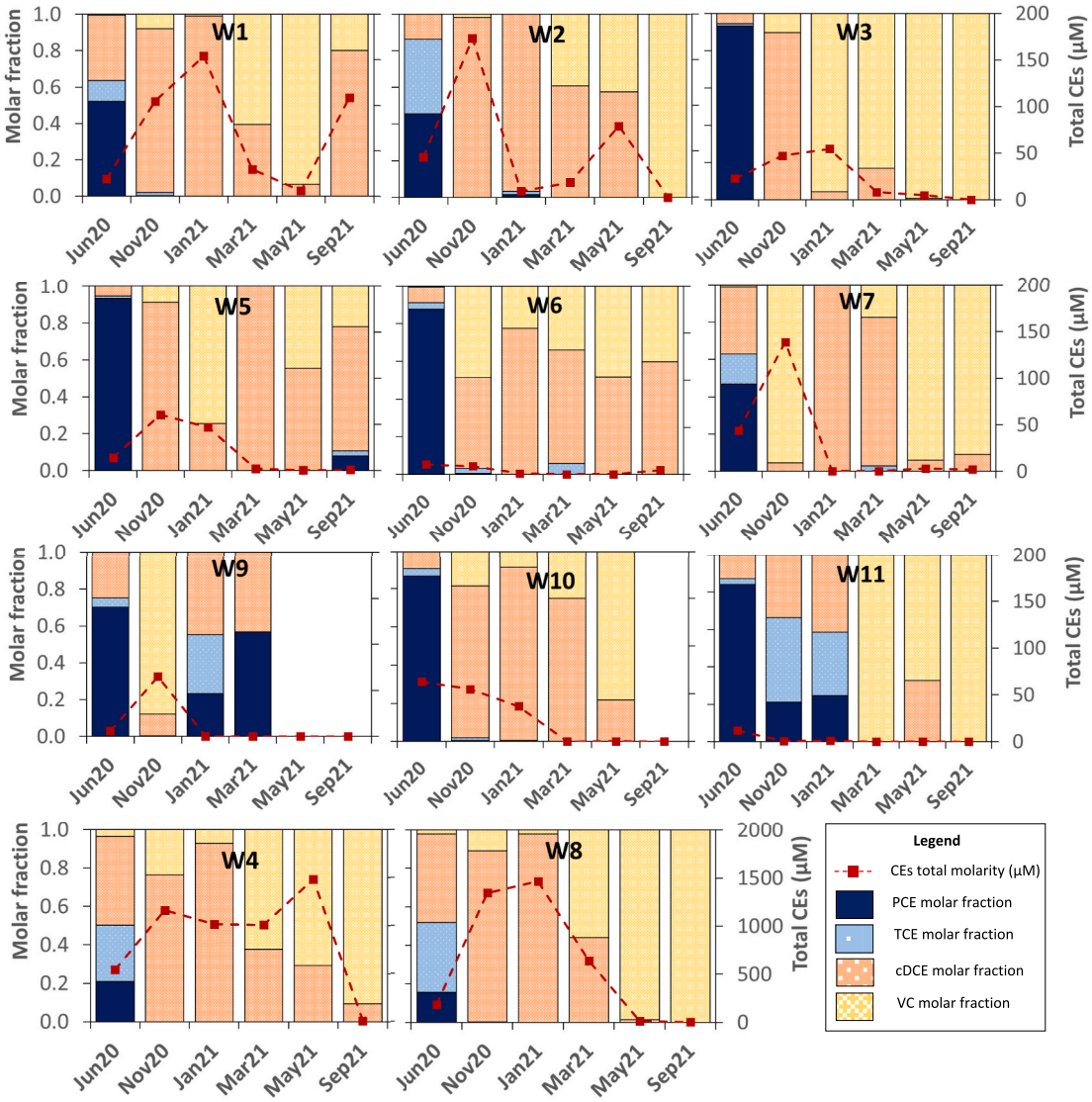

Fig. 4. 16-month evolution of CEs molar fractions in µM/µM (stacked charts) and total concentration of CEs (dashed lines) in the eleven monitored wells. First column shows the data of the sampling before the EVO injection. The following columns indicate molar fractions after injection.

population had increased significantly ($P < 0.05$), by 35-fold compared to the initial measurements, reaching values of 7.0 10^6 16S-Dhc mL^{-1}, while the functional gene populations also showed a substantial increase ($P < 0.05$): 8-fold higher for *tceA* (8.7 10^6 gene copies mL^{-1}), 1.4-fold for *bvcA* (4.1 10^5 gene copies mL^{-1}) and 5-fold for *vcrA* (6.1 10^6 gene copies mL^{-1}).

The expression of *tceA* and bvcA genes are associated with the transformation of cis-DCE to VC and VC to ethene, respectively, which is in agreement with the rise of the molar fraction of ethene in the microcosms (Fig. 3, Table 1). The functional gene *vcrA* can be associated with both cis-DCE and VC degradation (Lee et al., 2006; Blázquez-Pallí et al., 2019a; Franke et al., 2020). These results showed that Dhc populations and RD functional genes were good indicators of cis-DCE and VC biodegradation in the microcosm experiments performed.

In the field, the total bacterial population was heterogeneously distributed in the contaminated site before the injection of EVO, with values from different wells between 10^2 and 10^5 gene copies of 16S rRNA (see Table 1). The lowest bacterial population was observed in W11 well, while the highest ones were found in W4 and W10 wells (Fig. 1). This distribution was apparently neither related to initial CEs concentrations nor redox conditions. However, the lower 16S rRNA gene copies in W11 could have influenced the PCE and TCE slower biodegradation observed in this well. *Dhc* populations were present in all the wells before the EVO injection, with a maximum value of $1{\cdot}10^3$ gene copies mL^{-1} in W4. Previous studies indicated that *Dhc* populations in groundwater must exceed 10^4 copies mL^{-1} for acceptable RD to occur (Lu et al., 2006; Ernst, 2009; Ritalahti et al., 2010). Consequently, although the quantification of *Dhc* was indicative of the potential of bioremediation in the contaminated site, the *Dhc* population was not sufficient for effective natural attenuation. A different situation was observed six months after the EVO injection. Then, *Dhc* gene copies mL^{-1} above 10^4 were measured in all wells, reaching values up to 10^6 gene copies mL^{-1} in W8 and W10 ($P < 0.05$ compared to initial values in each well, Table 1). The amount of *Dhc* relative to the total bacterial population, between 0 and 2 % before the EVO injection, generally increased after the biostimulation reaching values above 10 % in W4 and 30 % in W8 wells. Only groundwater from the W4 well was analyzed in June 2021, but *Dhc* gene copies were still increasing, accounting for $1.95{\cdot}10^5$ *Dhc* $mL^{-1}$and suggesting that RD could be still ongoing.

Functional gene quantification was conducted in samples from W4 and W10 wells in June 2020 and March 2021, from W8 in March 2021 and from W4 in June 2021. Prior to the injection, (June 2020) functional

genes *tceA, bvcA* and *vcrA* were detected in W4 but not in W10. This result could explain the much higher molar fraction of cis-DCE and VC in W4 compared to W10 before the treatment. Six months after the EVO injection, *Dhc* population in W10 had increased by 5 orders of magnitude, and genes *tceA* and *vcrA* reached values of 10^6 copies mL^{-1}. However, *bvcA* gene copies remained lower than in the other wells (10^2 genes mL^{-1}). This could indicate that, although having the capacity for RD of TCE, the *Dhc* population in W10 well was different from those in W4 and W8, where the *bvcA* gene copies increased the same magnitude as *tceA* and *vcrA*. It is important to note that the number of copies of the *vcrA* gene in field samples is often higher than the total *Dhc* population. This may indicate that vcrABC cluster, typically found in *Dhc* genomic islands, could also be present in other OHRB by horizontal transfer or that this cluster is repeatedly present in *Dhc* genome as described by McMurdie et al. (2011).

Microbiological analyses of field samples were consistent with the results observed in the cis-DCE microcosm experiments. Microbiological field data also showed an increase in i) *Dhc* population relative to the total bacterial population and ii) functional genes related to RD (*tceA, bvcA* and *vcrA*). This suggests that the *Dhc* were most probably the drivers of RD in both the field and the microcosm experiments. Hence, the isotopic results obtained in the microcosm experiments might be representative for the analysis of biodegradation pathway and extent in the field.

3.5. Carbon and chlorine isotopic fractionation values and dual element isotope trends from the field-derived microcosms

In microcosm experiments, selected bottles were sacrificed at different extent of CEs degradation (Figs. S3, S4 and S5, in SI), water samples were collected for isotopic analysis and the isotopic fractionation ($\varepsilon^{13}C$ and $\varepsilon^{37}Cl$) for the RD of PCE, TCE and cis-DCE was determined according to Eq. (2) (Section 2.7). The carbon isotopic fractionation of VC was also estimated from the cis-DCE microcosms experiment using only the $\delta^{13}C_{VC}$ values of those samples where cis-DCE was already consumed (see SI). Given the fast degradation of PCE and TCE in both the microcosm experiments and in the contaminated site after the EVO injection (see above), cis-DCE was the predominant contaminant in the experiments (Fig. S2, in the SI) and in many wells during the investigated period (Fig. 4). Hereafter, the discussion of isotopic data from both the experiments and field samples is thus focussed on cis-DCE. The use of multi-element isotope data to investigate the fate of cis-DCE in the field is still very scarce in the literature (Zimmermann et al., 2020). The isotopic fractionation results for PCE, TCE ($\varepsilon^{13}C$ and $\varepsilon^{37}Cl$) and VC ($\varepsilon^{13}C$) and dual-element isotope slopes ($\Lambda^{C\text{-}Cl}$) for PCE and TCE in microcosm experiments are shown in the SI. All the εC, εCl and $\Lambda^{C/Cl}$ values calculated by OLR are summarised in Table 2. A comparison between Λ values and their uncertainties obtained in this study with the OLR and the York (Ojeda et al., 2019, 2020) regression methods is shown in the SI. Since no systematic bias introduced by ORL was observed and because there has not been sufficient time for the York method to be routinely adopted in 2D-CSIA studies, we used OLR values, but present York results in the SI.

Table 2
Calculated values of εC, εCl and $\Lambda^{C\text{-}Cl}$ for all compounds in the microcosm experiments and for cis-DCE in the field application. 95 % CI = 95 % confidence interval; N = number of points; n.a. = not analyzed.

	εC (‰)	95 % CI	εCl (‰)	95 % CI	$\Lambda^{C\text{-}Cl}$	95 % CI	N
Microcosms PCE	−1.1	0.7	−0.4	1.3	0.8	0.4	7
Microcosms TCE	−8	5	−2	1	5	1	8
Microcosms cis-DCE	−7	2	−1.5	0.4	4.9	0.8	14
Microcosms VC	−31	7	n.a.	n.a.	n.a.	n.a.	4
Field application cis-DCE	n.a.	n.a.	n.a.	n.a.	5	3	21

For cis-DCE, determined isotope fractionation values, i.e., $\varepsilon^{13}C = -7 \pm 2$ ‰ and $\varepsilon^{37}Cl = -1.5 \pm 0.4$ ‰, were lower than those reported in previous isotopic laboratory studies of anaerobic biodegradation of cis-DCE using pure and mixed cultures (Bloom et al., 2000; Abe et al., 2009; Fletcher et al., 2011; Kuder et al., 2013; Doğan-Subaşı et al., 2017; Lihl et al., 2019): from −31 to −14.9 ‰ ($n = 7$) and from −3.3 to −1.6 ‰ ($n = 5$) for $\varepsilon^{13}C$ and $\varepsilon^{37}Cl$, respectively. This suggests that despite following the same degradation pathway, isotope masking could significantly influence isotopic fractionation. Masking processes can be associated with the effect of rate-limiting (non or slightly isotope fractionating) steps preceding the bond cleavage such as contaminant mass transfer (Aeppli et al., 2009; Renpenning et al., 2015). Although considerable partitioning of the contaminant between the EVO and water phases, described in Section 3.1, might cause a mass transfer-related masking effect as reported by Aeppli et al., 2009, this effect can be discarded, as the microcosms did not contain an observable EVO phase and the injected amendment was lactate.

In contrast to single-element isotope fractionation analysis, combined shifts in isotope ratios of two elements in a dual-element isotope plot ($\Lambda^{C\text{-}Cl}$) should avoid the effect of isotope masking since the proportion of changes in isotope ratios of both elements relative to each other ($\Delta\delta^{13}C/\Delta\delta^{37}Cl$) is largely unaffected by nondegradative processes (Elsner, 2010; Thullner et al., 2013).

The dual-element isotope trend determined from microcosm experiments, i.e., $\Lambda^{C\text{-}Cl} = 4.9 \pm 0.8$ (Fig. 5) was lower than the range observed from previous laboratory studies with pure, enrichment and mixed cultures, i.e., between 8.3 and 17.8, $n = 4$ (Ojeda et al., 2020). However, the value obtained in this study agree well with the one reported in a previous study using field-derived microcosms, i.e. $\Lambda^{C\text{-}Cl} = 4.5 \pm 3.4$ (Doğan-Subaşı et al., 2017) (see further discussion below).

3.6. ^{13}C- and ^{37}Cl-CSIA of cis-DCE in field samples and dual-element isotope trend

In contrast to PCE and TCE, which were rapidly consumed in most of the wells, high fractions of cis-DCE were in general measured during the investigated period (Fig. 4), allowing the analysis of both carbon and chlorine isotopes in groundwater samples from all wells at multiple times.

The samples collected before the EVO injection (June 2020) showed cis-DCE $\delta^{13}C$ values ranging from −34.1 to −14.9 ‰ and most $\delta^{37}Cl$ values ranging between +2.7 and + 5.1 ‰. This isotopic pattern would reflect the formation of cis-DCE from the TCE, which is consistent with values reported by (Cretnik et al., 2014) and coherent with the high molar fractions of TCE and PCE in June 2020 (Fig. 4).

Conversely, the samples collected after the EVO injection showed in general a trend toward more positive $\delta^{13}C$ and $\delta^{37}Cl$ values (Fig. 5). Such enrichment in both ^{13}C and ^{37}Cl indicate the transformation of cis-DCE following the biostimulation treatment. In order to determine the dual-element isotope trend during cis-DCE transformation in the field after the EVO injection, $\delta^{13}C$ and $\delta^{37}Cl$ values were combined in Fig. 5. To avoid the effect of ongoing cis-DCE formation from RD of TCE, only isotopic data from those samples where PCE and TCE were not detected were considered ($n = 21$). As a result, a $\Lambda^{C\text{-}Cl}$ value of 5 ± 3 was determined for the field (Fig. 5), which is very similar to the value obtained from the laboratory experiments performed in this study ($\Lambda^{C\text{-}Cl} = 4.9 \pm 0.8$). This result indicates that microbial RD of cis-DCE via hydrogenolysis to VC was the main reaction mechanism controlling the fate of cis-DCE at the site after the EVO injection. These results agree with the detection of VC (molar fraction >5 %) in all selected samples.

It is interesting to note that despite microbiological data pointed to *Dhc* bacteria as the most likely responsible for RD of cis-DCE in both the field site and microcosm experiments (see above), reported $\Lambda^{C\text{-}Cl}$ values for microbial RD of cis-DCE by *Dhc* strains (i.e., *D. mccartyi* strain BTF08, 18 ± 1, strain 195, 10.0 ± 0.4 (Lihl et al., 2019)) and mixed cultures

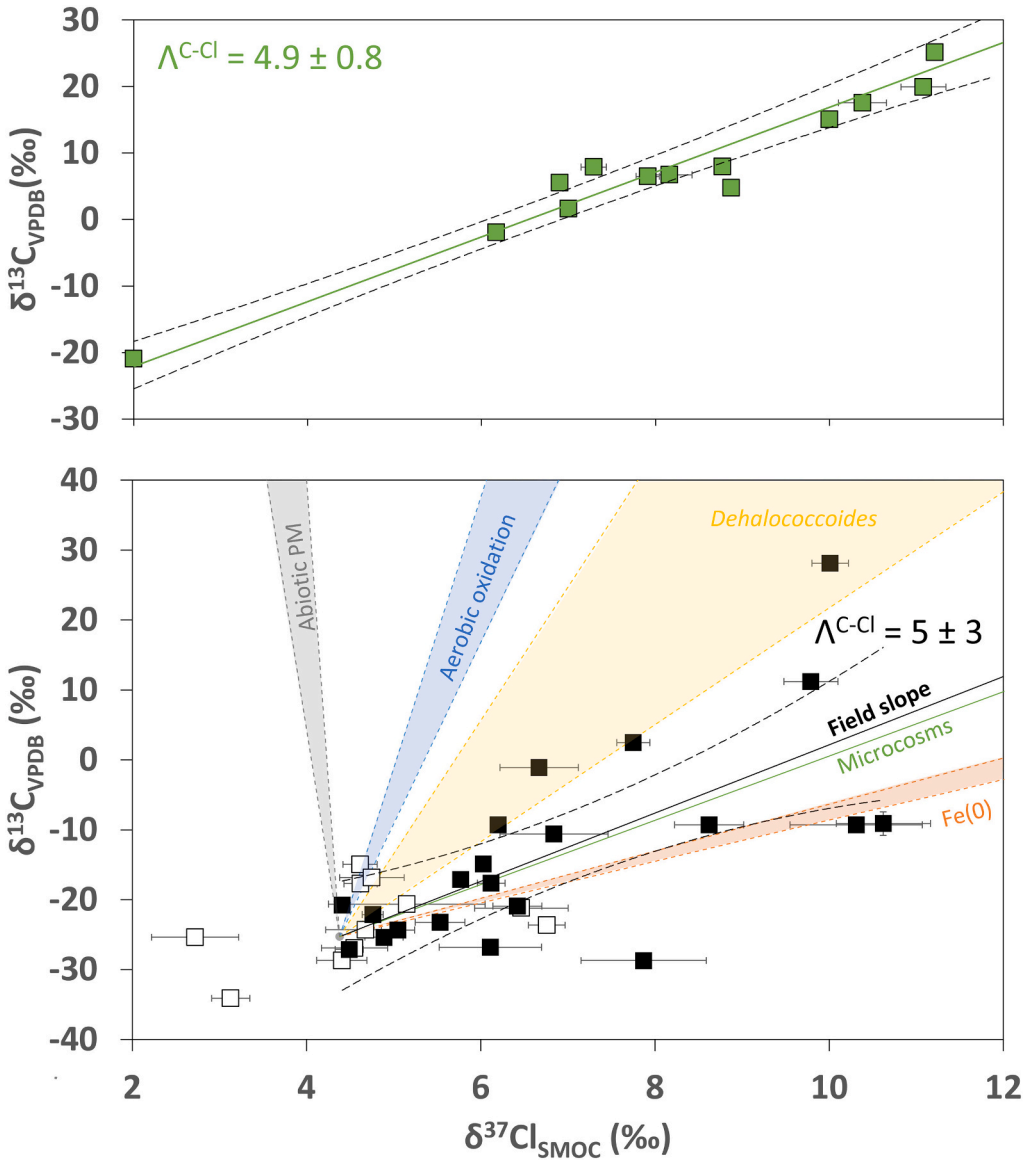

Fig. 5. Dual element C-Cl isotope plot of cis-DCE from samples of the microcosm experiments (upper panel) and the field (lower panel). Λ values (±95 % C.I.) are given by the slope of the linear regressions and the black dashed lines correspond to the 95 % C.I. Error bars for $\delta^{13}C$ values are generally smaller than the symbols. In the lower panel, the empty markers represent data from samples collected prior to the injection, while filled black markers correspond to those measured after the EVO injection. The green line represents the slope obtained from the microcosm experiments in this study and the colored areas correspond to ranges of previously reported slopes for different degradation processes: grey for abiotic oxidation by permanganate (Doğan-Subaşı et al., 2017), blue for aerobic oxidation (Abe et al., 2009), yellow for reductive dechlorination in *Dhc* cultures (Bloom et al., 2000; Abe et al., 2009; Fletcher et al., 2011; Kuder et al., 2013; Lihl et al., 2019), and orange for abiotic degradation with Fe(0) (Audí-Miró et al., 2013).

containing *Dhc* spp. (8.3 (Kuder et al., 2013) and 11.4 ± 0.6 (Abe et al., 2009)) were higher than those determined in this study (Fig. 5). This difference might be related with distinct reaction mechanisms and/or the use of different Rdhs during RD of cis-DCE by *Dhc* bacteria. Discrepancies on $\Lambda^{C\text{-}Cl}$ values, especially when small isotopic fractionation is observed for both carbon and chlorine, might not always reflect the chemical reaction mechanism, but preceding rate-limiting steps during enzyme – substrate association or enzymatic structure, as previously reported for other compounds such as PCE (Renpenning et al., 2014), TCE (Gafni et al., 2020) and trichloromethane (Heckel et al., 2019). Further research will be necessary to unravel the mechanisms behind these observed differences for RD of cis-DCE. Nevertheless, the slope determined in this study from field samples is strongly different compared to that determined for aerobic oxidation (32 ± 6, Abe et al. (2009)), indicating a non-significant biodegradation of cis-DCE under oxic conditions during the EISB treatment (Fig. 5).

Finally, for abiotic degradation processes, the starkly contrasting slope determined for oxidation by permanganate, −125 ± 47 (Doğan-Subaşı et al., 2017), will allow to differentiate between abiotic oxidation and microbial RD of cis-DCE in applications of in situ chemical oxidation by permanganate. However, for cis-DCE dichloroelimination by Fe(0) (via single electron transfer), a value relatively close to the slope of 5 ± 3 obtained in this study (Fig. 5) was reported (i.e. 3.1 ± 0.2 (Audí-Miró et al., 2013)), which could make it difficult to differentiate between cis-DCE transformation by microbial and abiotic RD in engineered remediation treatments such as Fe(0) permeable reactive barriers. In summary, the results of this study show the potential of a dual-element isotope approach to investigate transformation processes of cis-DCE in remediation of contaminated sites by EISB with EVO.

4. Conclusions

This study shows the potential of a multi-method approach for evaluating EISB of CEs with EVO in a contaminated site. Microbiological analyses indicated a significant increase in *Dhc* populations and RD functional genes in cis-DCE microcosms and the field, pointing to *Dhc* bacteria as the most likely responsible for RD of cis-DCE. The dual-element (C, Cl) isotope analysis showed similar $\Lambda^{C\text{-}Cl}$ values for i) the laboratory experiment of RD of cis-DCE and ii) the field samples collected after the EVO injection, i.e., 4.9 ± 0.8 and 5 ± 3, respectively, indicating that the fate of cis-DCE in the field was controlled by its transformation (hydrogenolysis) to VC. This result highlights the potential of the dual-element isotope approach to link the transformation processes determined in the laboratory experiments with those occurring in the field.

However, the $\Lambda^{C\text{-}Cl}$ values for RD of cis-DCE determined in this study from field-derived microcosm experiments and field samples (around 5.0) differ from those reported so far for laboratory studies with *Dhc* strains and mixed cultures containing *Dhc*., i.e., between 17.8 and 8.3 (Ojeda et al., 2020). This observation underscores the importance of determining site-specific Λ and ε values from derived microcosm experiments in order to improve the identification and quantification of transformation processes in contaminated sites using isotope data. In addition, the experiments of water – EVO phase partitioning of CEs showed, for the first time, that despite their high partitioning into the EVO, the effect on the carbon isotope ratios of CEs would be small or insignificant compared to that caused by biodegradation of the CEs in the groundwater in a field application scale.

The results of this study provide valuable insight for the practical application of dual isotopic (C, Cl) and biomolecular tools to i) assess degradation pathways of CEs, especially cis-DCE, in contaminated sites by EISB with EVO and ii) improve the understanding of the complex interactions among EVO, contaminant concentrations, and microbial communities in future field studies.

Funding

This study was financed through the following projects: INNOTECRD19-1-0006 funded by ACCIÓ, PACE-ISOTEC (CGL2017-87216-C4-1-R) financed by the Spanish Government and AEI/FEDER from the UE and the Consolidated Research Group MAGH project (2021-SGR-00308), financed by the AGAUR (Catalan Government). The experiments and work performed by S. Gil-Villalba were supported by the FPI2018/084979 contract, and the IAGC Student Research Grant (2022).

CRediT authorship contribution statement

Sergio Gil-Villalba: Writing – original draft, Methodology, Investigation, Formal analysis, Data curation. **Jordi Palau:** Writing – review & editing, Visualization, Validation, Supervision, Project administration, Methodology, Investigation, Conceptualization. **Jesica M. Soder-Walz:** Writing – review & editing, Supervision, Methodology, Investigation. **Miguel A. Vallecillo:** Validation, Supervision, Project administration, Methodology. **Jordi Corregidor:** Validation, Project administration, Methodology. **Andrea Tirado:** Methodology, Data curation. **Orfan Shouakar-Stash:** Validation, Supervision, Methodology, Investigation, Formal analysis. **Miriam Guivernau:** Writing – review & editing, Visualization, Methodology, Investigation, Data curation. **Marc Viñas:** Writing – review & editing, Validation, Supervision, Methodology. **Albert Soler:** Validation, Supervision, Resources, Funding acquisition, Conceptualization. **Monica Rosell:** Writing – review & editing, Visualization, Validation, Supervision, Project administration, Methodology, Investigation, Conceptualization.

Declaration of competing interest

The authors declare that they have no known competing financial interests or personal relationships that could have appeared to influence the work reported in this paper.

Data availability

Data will be made available on request.

Acknowledgements

We thank Anna Rigol from Department of Chemical Engineering and Analytical Chemistry, Faculty of Chemistry, in UB for providing us with the idea and the dialysis membrane for separating EVO from the water solution. We thank all technicians in MAiMA and CCiT-UB for their support. We truly appreciate all the constructive comments and suggestions from the three reviewers that have considerably improved our manuscript.

Appendix A. Supplementary data

Supplementary data to this article can be found online at https://doi.org/10.1016/j.scitotenv.2024.175351.

References

Abe, Y., Aravena, R., Zopfi, J., Shouakar-Stash, O., Cox, E., Roberts, J.D., Hunkeler, D., 2009. Carbon and chlorine isotope fractionation during aerobic oxidation and reductive dechlorination of vinyl chloride and cis-1, 2-dichloroethene. Environ. Sci. Technol. 43 (1), 101–107. https://doi.org/10.1021/es801759k.

Aelion, C.M., Höhener, P., Hunkeler, D., Aravena, R., 2009. Environmental isotopes in biodegradation and bioremediation. In: Environmental Isotopes in Biodegradation and Bioremediation. https://doi.org/10.1201/9781420012613.

Aeppli, C., Berg, M., Cirpka, O.A., Holliger, C., Schwarzenbach, R.P., Hofstetter, T.B., 2009. Influence of mass-transfer limitations on carbon isotope fractionation during microbial dechlorination of trichloroethene. Environ. Sci. Technol. 43 (23), 8813–8820. https://doi.org/10.1021/es901481b.

ATSDR, 2023. Substance Priority List [WWW Document]. Subst. Prior, List. https://www.atsdr.cdc.gov/spl/index.html#2022spl.

Audí-Miró, C., Cretnik, S., Otero, N., Palau, J., Shouakar-Stash, O., Soler, A., Elsner, M., 2013. Cl and C isotope analysis to assess the effectiveness of chlorinated ethene degradation by zero-valent iron: evidence from dual element and product isotope values. Appl. Geochem. 32, 175–183. https://doi.org/10.1016/j.apgeochem.2012.08.025.

Badin, A., Buttet, G., Maillard, J., Holliger, C., Hunkeler, D., 2014. Multiple dual C-Cl isotope patterns associated with reductive dechlorination of tetrachloroethene. Environ. Sci. Technol. 48 (16), 9179–9186. https://doi.org/10.1021/es500822d.

Bernstein, A., Shouakar-Stash, O., Ebert, K., Laskov, C., Hunkeler, D., Jeannottat, S., Sakaguchi-Söder, K., Laaks, J., Jochmann, M.A., Cretnik, S., Jager, J., Haderlein, S. B., Schmidt, T.C., Aravena, R., Elsner, M., 2011. Compound-specific chlorine isotope analysis: a comparison of gas chromatography/isotope ratio mass spectrometry and gas chromatography/quadrupole mass spectrometry methods in an Interlaboratory study. Anal. Chem. 83 (20), 7624–7634. https://doi.org/10.1021/ac200516c.

Blázquez-Pallí, N., Rosell, M., Varias, J., Bosch, M., Soler, A., Vicent, T., Marco-Urrea, E., 2019a. Multi-method assessment of the intrinsic biodegradation potential of an aquifer contaminated with chlorinated ethenes at an industrial area in Barcelona (Spain). Environ. Pollut. 244, 165–173. https://doi.org/10.1016/j.envpol.2018.10.013.

Blázquez-Pallí, N., Shouakar-Stash, O., Palau, J., Trueba-Santiso, A., Varias, J., Bosch, M., Soler, A., Vicent, T., Marco-Urrea, E., Rosell, M., 2019b. Use of dual element isotope analysis and microcosm studies to determine the origin and potential anaerobic biodegradation of dichloromethane in two multi-contaminated aquifers. Sci. Total Environ. 696, 134066 https://doi.org/10.1016/j.scitotenv.2019.134066.

Bloom, Y., Aravena, R., Hunkeler, D., Edwards, E., Frape, S.K., 2000. Carbon isotope fractionation during microbial dechlorination of trichloroethene, cis-l,2-dichloroethene, and vinyl chloride: implications for assessment of natural attenuation. Environ. Sci. Technol. 34 (13), 2768–2772. https://doi.org/10.1021/es991179k.

Chen, G., Kara Murdoch, F., Xie, Y., Murdoch, R.W., Cui, Y., Yang, Y., Yan, J., Key, T.A., Löffler, F.E., 2022b. Dehalogenation of Chlorinated Ethenes to Ethene by a Novel Isolate, "Candidatus Dehalogenimonas etheniformans". Appl. Environ. Microbiol. 88 (12) https://doi.org/10.1128/aem.00443-22.

Chen, W., Chen, K., Surmpalli, R.Y., Zhang, T.C., Ou, J., Kao, C., 2022a. Bioremediation of trichloroethylene-polluted groundwater using emulsified castor oil for slow carbon release and acidification control. Water Environ. Res. 94 (1) https://doi.org/10.1002/wer.1673.

Coplen, T.B., 1996. New guidelines for reporting stable hydrogen, carbon, and oxygen isotope-ratio data. Geochim. Cosmochim. Acta 60 (17), 3359–3360. https://doi.org/10.1016/0016-7037(96)00263-3.

Coplen, T.B., 2011. Guidelines and recommended terms for expression of stable-isotope-ratio and gas-ratio measurement results. Rapid Commun. Mass Spectrom. 25 (17), 2538–2560. https://doi.org/10.1002/rcm.5129.

Cretnik, S., Bernstein, A., Shouakar-Stash, O., Löffler, F., Elsner, M., 2014. Chlorine isotope effects from isotope ratio mass spectrometry suggest intramolecular C-Cl bond competition in trichloroethene (TCE) reductive dehalogenation. Molecules 19 (5), 6450–6473. https://doi.org/10.3390/molecules19056450.

Doğan-Subaşı, E., Elsner, M., Qiu, S., Cretnik, S., Atashgahi, S., Shouakar-Stash, O., Boon, N., Dejonghe, W., Bastiaens, L., 2017. Contrasting dual (C, Cl) isotope fractionation offers potential to distinguish reductive chloroethene transformation from breakdown by permanganate. Sci. Total Environ. 596–597, 169–177. https://doi.org/10.1016/j.scitotenv.2017.03.292.

Duhamel, M., Wehr, S.D., Yu, L., Rizvi, H., Seepersad, D., Dworatzek, S., Cox, E.E., Edwards, E.A., 2002. Comparison of anaerobic dechlorinating enrichment cultures maintained on tetrachloroethene, trichloroethene, cis -dichloroethene and vinyl chloride. Water Res. 36, 4193–4202.

Elsner, M., 2010. Stable isotope fractionation to investigate natural transformation mechanisms of organic contaminants: principles, prospects and limitations. J. Environ. Monit. 12 (11), 2005–2031. https://doi.org/10.1039/c0em00277a.

Ernst, T.J., 2009. Use of "Dehalococcoides" to bioremediate groundwater contaminated with chlorinated solvents. Basic Biotechnol. eJournal 5 (1), 72–77.

Fletcher, K.E., Nijenhuis, I., Richnow, H.H., Löffler, F.E., 2011. Stable carbon isotope enrichment factors for cis -1,2-dichloroethene and vinyl chloride reductive dechlorination by dehalococcoides. Environ. Sci. Technol. 45 (7), 2951–2957. https://doi.org/10.1021/es103728q.

Franke, S., Seidel, K., Adrian, L., Nijenhuis, I., 2020. Dual element (C/Cl) isotope analysis indicates distinct mechanisms of reductive dehalogenation of chlorinated ethenes and dichloroethane in dehalococcoides mccartyi strain BTF08 with defined reductive dehalogenase inventories. Front. Microbiol. 11 (July) https://doi.org/10.3389/fmicb.2020.01507.

Gafni, A., Gelman, F., Ronen, Z., Bernstein, A., 2020. Variable carbon and chlorine isotope fractionation in TCE co-metabolic oxidation. Chemosphere 242. https://doi.org/10.1016/j.chemosphere.2019.125130.

Halloran, L.J.S., Vakili, F., Wanner, P., Shouakar-Stash, O., Hunkeler, D., 2021. Sorption- and diffusion-induced isotopic fractionation in chloroethenes. Sci. Total Environ. 788, 147826 https://doi.org/10.1016/j.scitotenv.2021.147826.

Harkness, M., 2000. Economic considerations in enhanced anaerobic biodegradation. In: Bioremediation and Phytoremediation of Chlorinated and Recalcitrant Compounds, pp. 9–14.

Harkness, M., Fisher, A., 2013. Use of emulsified vegetable oil to support bioremediation of TCE DNAPL in soil columns. J. Contam. Hydrol. 151, 16–33. https://doi.org/10.1016/j.jconhyd.2013.04.002.

He, J., Sung, Y., Krajmalnik-Brown, R., Ritalahti, K.M., Löffler, F.E., 2005. Isolation and characterization of Dehalococcoides sp. strain FL2, a trichloroethene (TCE)- and 1,2-dichloroethene-respiring anaerobe. Environ. Microbiol. 7 (9), 1442–1450. https://doi.org/10.1111/j.1462-2920.2005.00830.x.

Heckel, B., Phillips, E., Edwards, E., Sherwood Lollar, B., Elsner, M., Manefield, M.J., Lee, M., 2019. Reductive dehalogenation of Trichloromethane by two different *Dehalobacter restrictus* strains reveal opposing dual element isotope effects. Environ. Sci. Technol. 53 (5), 2332–2343. https://doi.org/10.1021/acs.est.8b03717.

Hermon, L., Denonfoux, J., Hellal, J., Joulian, C., Ferreira, S., Vuilleumier, S., Imfeld, G., 2018. Dichloromethane biodegradation in multi-contaminated groundwater: insights from biomolecular and compound-specific isotope analyses. Water Res. 142, 217–226. https://doi.org/10.1016/j.watres.2018.05.057.

Hiortdahl, K.M., Borden, R.C., 2014. Enhanced reductive dechlorination of tetrachloroethene dense nonaqueous phase liquid with EVO and $Mg(OH)_2$. Environ. Sci. Technol. 48 (1), 624–631. https://doi.org/10.1021/es4042379.

Hirschorn, S.K., Grostern, A., Lacrampe-Couloume, G., Edwards, E.A., MacKinnon, L., Repta, C., Major, D.W., Sherwood Lollar, B., 2007. Quantification of biotransformation of chlorinated hydrocarbons in a biostimulation study: added value via stable carbon isotope analysis. J. Contam. Hydrol. 94 (3–4), 249–260. https://doi.org/10.1016/j.jconhyd.2007.07.001.

Höhener, P., Yu, X., 2012. Stable carbon and hydrogen isotope fractionation of dissolved organic groundwater pollutants by equilibrium sorption. J. Contam. Hydrol. 129–130, 54–61. https://doi.org/10.1016/j.jconhyd.2011.09.006.

Hug, L.A., 2016. In: Adrian, L., Löffler, F.E. (Eds.), Diversity, Evolution, and Environmental Distribution of Reductive Dehalogenase Genes BT - Organohalide-Respiring Bacteria. Springer, Berlin Heidelberg, pp. 377–393. https://doi.org/10.1007/978-3-662-49875-0_16.

Jin, B., Laskov, C., Rolle, M., Haderlein, S.B., 2011. Chlorine isotope analysis of organic contaminants using GC-qMS: method optimization and comparison of different evaluation schemes. Environ. Sci. Technol. 45 (12), 5279–5286. https://doi.org/10.1021/es200749d.

Kaufmann, R., Long, A., Bentley, H., Davis, S., 1984. Natural chlorine isotope variations. Nature 309 (5966), 338–340. https://doi.org/10.1038/309338a0.

Kuder, T., Philp, P., 2013. Demonstration of compound-specific isotope analysis of hydrogen isotope ratios in chlorinated ethenes. Environ. Sci. Technol. 47 (3), 1461–1467. https://doi.org/10.1021/es303476v.

Kuder, T., Van Breukelen, B.M., Vanderford, M., Philp, P., 2013. 3D-CSIA: carbon, chlorine, and hydrogen isotope fractionation in transformation of TCE to ethene by a dehalococcoides culture. Environ. Sci. Technol. 47 (17), 9668–9677. https://doi.org/10.1021/es400463p.

Lalman, J.A., Bagley, D.M., 2000. Anaerobic degradation and inhibitory effects of linoleic acid. Water Res. 34 (17), 4220–4228. https://doi.org/10.1016/S0043-1354(00)00180-9.

Lee, P.K.H., Johnson, D.R., Holmes, V.F., He, J., Alvarez-Cohen, L., 2006. Reductive dehalogenase gene expression as a biomarker for physiological activity of *Dehalococcoides* spp. Appl. Environ. Microbiol. 72 (9), 6161–6168. https://doi.org/10.1128/AEM.01070-06.

Lee, P.K.H., Macbeth, T.W., Sorenson, K.S., Deeb, R.A., Alvarez-Cohen, L., 2008. Quantifying genes and transcripts to assess the in situ physiology of "*Dehalococcoides*" spp. in a trichloroethene-contaminated groundwater site. Appl. Environ. Microbiol. 74 (9), 2728–2739. https://doi.org/10.1128/AEM.02199-07.

Lee, Y.-C., Kwon, T.-S., Yang, J.-S., Yang, J.-W., 2007. Remediation of groundwater contaminated with DNAPLs by biodegradable oil emulsion. J. Hazard. Mater. 140 (1), 340–345. https://doi.org/10.1016/j.jhazmat.2006.09.036.

Leeson, A., Beevar, E., Henry, B., Fortenberry, J., Coyle, C., 2004. Microbiological and geochemical considerations. In: Principles and Practices of Enhanced Anaerobic Bioremdiation of Chlorinated Solvents, Section 2, pp. 2-1–2-11.

Lihl, C., Douglas, L.M., Franke, S., Pérez-De-Mora, A., Meyer, A.H., Daubmeier, M., Edwards, E.A., Nijenhuis, I., Sherwood Lollar, B., Elsner, M., 2019. Mechanistic dichotomy in bacterial trichloroethene dechlorination revealed by carbon and chlorine isotope effects. Environ. Sci. Technol. 53 (8), 4245–4254. https://doi.org/10.1021/acs.est.8b06643.

Löffler, F.E., Ritalahti, K.M., Zinder, S.H., 2013. In: Stroo, H.F., Leeson, A., Ward, C.H. (Eds.), Dehalococcoides and reductive Dechlorination of chlorinated solvents BT - bioaugmentation for groundwater remediation. Springer, New York, pp. 39–88. https://doi.org/10.1007/978-1-4614-4115-1_2.

Long, C.M., Borden, R.C., 2006. Enhanced reductive dechlorination in columns treated with edible oil emulsion. J. Contam. Hydrol. 87 (1), 54–72. https://doi.org/10.1016/j.jconhyd.2006.04.010.

Lu, X., Wilson, J.T., Kampbell, D.H., 2006. Relationship between Dehalococcoides DNA in ground water and rates of reductive dechlorination at field scale. Water Res. 40 (16), 3131–3140. https://doi.org/10.1016/j.watres.2006.05.030.

Magnuson, J.K., Romine, M.F., Burris, D.R., Kingsley, M.T., 2000. Trichloroethene reductive dehalogenase from *Dehalococcoides ethenogenes*: sequence of tceA and substrate range characterization. Appl. Environ. Microbiol. 66 (12), 5141–5147. https://doi.org/10.1128/AEM.66.12.5141-5147.2000.

McMurdie, P.J., Hug, L.A., Edwards, E.A., Holmes, S., Spormann, A.M., 2011. Site-specific mobilization of vinyl chloride Respiration Islands by a mechanism common in Dehalococcoides. BMC Genom. 12 (1), 287. https://doi.org/10.1186/1471-2164-12-287.

Newman, W.A., Pelle, R.C., 2006. Enhanced anaerobic bioremediation of chlorinated solvents utilizing vegetable oil emulsions. Remediation 16 (3), 109–122. https://doi.org/10.1002/rem.20095.

Ni, S., Fredrickson, J.K., Xun, L., 1995. Purification and characterization of a novel 3-chlorobenzoate-reductive dehalogenase from the cytoplasmic membrane of *Desulfomonile tiedjei* DCB-1. J. Bacteriol. 177 (17), 5135–5139. https://doi.org/10.1128/jb.177.17.5135-5139.1995.

Nijenhuis, I., Nikolausz, M., Köth, A., Felföldi, T., Weiss, H., Drangmeister, J., Großmann, J., Kästner, M., Richnow, H.H., 2007. Assessment of the natural attenuation of chlorinated ethenes in an anaerobic contaminated aquifer in the Bitterfeld/Wolfen area using stable isotope techniques, microcosm studies and molecular biomarkers. Chemosphere 67 (2), 300–311. https://doi.org/10.1016/j.chemosphere.2006.09.084.

Nijenhuis, I., Renpenning, J., Kümmel, S., Richnow, H.H., Gehre, M., 2016. Recent advances in multi-element compound-specific stable isotope analysis of organohalides: achievements, challenges and prospects for assessing environmental sources and transformation. Trends Environ. Anal. Chem. 11, 1–8. https://doi.org/10.1016/j.teac.2016.04.001.

Ojeda, A.S., Phillips, E., Mancini, S.A., Lollar, B.S., 2019. Sources of uncertainty in biotransformation mechanistic interpretations and remediation studies using CSIA. Anal. Chem. 91 (14), 9147–9153. https://doi.org/10.1021/acs.analchem.9b01756.

Ojeda, A.S., Phillips, E., Sherwood Lollar, B., 2020. Multi-element (C, H, Cl, Br) stable isotope fractionation as a tool to investigate transformation processes for halogenated hydrocarbons. Environ. Sci.: Processes Impacts 22 (3), 567–582. https://doi.org/10.1039/C9EM00498J.

Palau, J., Soler, A., Teixidor, P., Aravena, R., 2007. Compound-specific carbon isotope analysis of volatile organic compounds in water using solid-phase microextraction. J. Chromatogr. A 1163 (1), 260–268. https://doi.org/10.1016/j.chroma.2007.06.050.

Palau, J., Marchesi, M., Chambon, J.C.C., Aravena, R., Canals, À., Binning, P.J., Bjerg, P. L., Otero, N., Soler, A., 2014. Multi-isotope (carbon and chlorine) analysis for fingerprinting and site characterization at a fractured bedrock aquifer contaminated by chlorinated ethenes. Sci. Total Environ. 475, 61–70. https://doi.org/10.1016/j.scitotenv.2013.12.059.

Pfeiffer, P., Bielefeldt, A.R., Illangasekare, T., Henry, B., 2005. Partitioning of dissolved chlorinated ethenes into vegetable oil. Water Res. 39 (18), 4521–4527. https://doi.org/10.1016/j.watres.2005.09.016.

Renpenning, J., Keller, S., Cretnik, S., Shouakar-Stash, O., Elsner, M., Schubert, T., Nijenhuis, I., 2014. Combined C and Cl isotope effects indicate differences between corrinoids and enzyme (*Sulfurospirillum multivorans* PceA) in reductive dehalogenation of tetrachloroethene, but not trichloroethene. Environ. Sci. Technol. 48 (20), 11837–11845. https://doi.org/10.1021/es503306g.

Renpenning, J., Rapp, I., Nijenhuis, I., 2015. Substrate hydrophobicity and cell composition influence the extent of rate limitation and masking of isotope fractionation during microbial reductive dehalogenation of chlorinated Ethenes. Environ. Sci. Technol. 49 (7), 4293–4301. https://doi.org/10.1021/es506108j.

Révész, K.M., Lollar, B.S., Kirshtein, J.D., Tiedeman, C.R., Imbrigiotta, T.E., Goode, D.J., Shapiro, A.M., Voytek, M.A., Lacombe, P.J., Busenberg, E., 2014. Integration of stable carbon isotope, microbial community, dissolved hydrogen gas, and $^{2}HH_2O$ tracer data to assess bioaugmentation for chlorinated ethene degradation in fractured rocks. J. Contam. Hydrol. 156, 62–77. https://doi.org/10.1016/j.jconhyd.2013.10.004.

Ritalahti, K.M., Hatt, J.K., Lugmayr, V., Henn, K., Petrovskis, E.A., Ogles, D.M., Davis, G. A., Yeager, C.M., Lebrón, C.A., Löffler, F.E., 2010. Comparing on-site to off-site biomass collection for Dehalococcoides biomarker gene quantification to predict in situ chlorinated Ethene detoxification potential. Environ. Sci. Technol. 44 (13), 5127–5133. https://doi.org/10.1021/es100408r.

Rodríguez-Fernández, D., Heckel, B., Torrentó, C., Meyer, A., Elsner, M., Hunkeler, D., Soler, A., Rosell, M., Domènech, C., 2018. Dual element (C-Cl) isotope approach to distinguish abiotic reactions of chlorinated methanes by Fe(0) and by Fe(II) on iron minerals at neutral and alkaline pH. Chemosphere 206, 447–456. https://doi.org/10.1016/j.chemosphere.2018.05.036.

Rosell, M., Palau, J., Mortan, S.H., Caminal, G., Soler, A., Shouakar-Stash, O., Marco-Urrea, E., 2019. Dual carbon - chlorine isotope fractionation during dichloroelimination of 1,1,2-trichloroethane by an enrichment culture containing *Dehalogenimonas* sp. Sci. Total Environ. 648, 422–429. https://doi.org/10.1016/j.scitotenv.2018.08.071.

Shouakar-Stash, O., Drimmie, R.J., Zhang, M., Frape, S.K., 2006. Compound-specific chlorine isotope ratios of TCE, PCE and DCE isomers by direct injection using CF-IRMS. Appl. Geochem. 21 (5), 766–781. https://doi.org/10.1016/j.apgeochem.2006.02.006.

Thullner, M., Fischer, A., Richnow, H.-H., Wick, L.Y., 2013. Influence of mass transfer on stable isotope fractionation. Appl. Microbiol. Biotechnol. 97 (2), 441–452. https://doi.org/10.1007/s00253-012-4537-7.

Tiehm, A., Schmidt, K.R., 2011. Sequential anaerobic/aerobic biodegradation of chloroethenes-aspects of field application. Curr. Opin. Biotechnol. 22 (3), 415–421. https://doi.org/10.1016/j.copbio.2011.02.003.

Torrentó, C., Palau, J., Rodríguez-Fernández, D., Heckel, B., Meyer, A., Domènech, C., Rosell, M., Soler, A., Elsner, M., Hunkeler, D., 2017. Carbon and chlorine isotope fractionation patterns associated with different engineered chloroform transformation reactions. Environ. Sci. Technol. 51 (11), 6174–6184. https://doi.org/10.1021/acs.est.7b00679.

Underwood, J.C., Akob, D.M., Lorah, M.M., Imbrigiotta, T.E., Harvey, R.W., Tiedeman, C.R., 2022. Microbial community response to a bioaugmentation test to degrade trichloroethylene in a fractured rock aquifer, Trenton, N.J. FEMS Microbiol. Ecol. 98 (7), fiac077 https://doi.org/10.1093/femsec/fiac077.

Wanner, P., Parker, B.L., Chapman, S.W., Aravena, R., Hunkeler, D., 2017. Does sorption influence isotope ratios of chlorinated hydrocarbons under field conditions? Appl. Geochem. 84, 348–359. https://doi.org/10.1016/j.apgeochem.2017.07.016.

West, K.A., Lee, P.K.H., Johnson, D.R., Zinder, S.H., Alvarez-Cohen, L., 2013. Global gene expression of Dehalococcoides within a robust dynamic TCE-dechlorinating community under conditions of periodic substrate supply. Biotechnol. Bioeng. 110 (5), 1333–1341. https://doi.org/10.1002/bit.24819.

Wiegert, C., Aeppli, C., Knowles, T., Holmstrand, H., Evershed, R., Pancost, R.D., Macháčková, J., Gustafsson, Ö., 2012. Dual carbon-chlorine stable isotope investigation of sources and fate of chlorinated ethenes in contaminated groundwater. Environ. Sci. Technol. 46 (20), 10918–10925. https://doi.org/10.1021/es3016843.

Yang, Y., Mccarty, P.L., 2000. Biologically enhanced dissolution of tetrachloroethene DNAPL. Environ. Sci. Technol. 34 (14), 2979–2984. https://doi.org/10.1021/es991410u.

Yu, R., Andrachek, R.G., Lehmicke, L.G., Freedman, D.L., 2018. Remediation of chlorinated ethenes in fractured sandstone by natural and enhanced biotic and abiotic processes: a crushed rock microcosm study. Sci. Total Environ. 626, 497–506. https://doi.org/10.1016/j.scitotenv.2018.01.064.

van der Zaan, B., Hannes, F., Hoekstra, N., Rijnaarts, H., de Vos, W.M., Smidt, H., Gerritse, J., 2010. Correlation of *Dehalococcoides* 16S rRNA and chloroethene-reductive dehalogenase genes with geochemical conditions in chloroethene-contaminated groundwater. Appl. Environ. Microbiol. 76 (3), 843–850. https://doi.org/10.1128/AEM.01482-09.

Zimmermann, J., Halloran, L.J.S., Hunkeler, D., 2020. Tracking chlorinated contaminants in the subsurface using compound-specific chlorine isotope analysis: a review of principles, current challenges and applications. Chemosphere 244, 125476. https://doi.org/10.1016/j.chemosphere.2019.125476.